Journal of Chromatography A, 1217 (2010) 7074–7081

Contents lists available at ScienceDirect

Journal of Chromatography A

journal homepage: www.elsevier.com/locate/chroma

Relationship between the particle size distribution of commercial fully porous and superficially porous high-performance liquid chromatography column packings and their chromatographic performance

D. Cabooter[a,*], A. Fanigliulo[b], G. Bellazzi[b], B. Allieri[b], A. Rottigni[b], G. Desmet[a]

[a] Vrije Universiteit Brussel, Department of Chemical Engineering, Pleinlaan 2, 1050 Brussels, Belgium
[b] GlaxoSmithKline R&D, Pharmaceutical Development, Via Fleming 4, 37135 Verona, Italy

ARTICLE INFO

Article history:
Received 24 June 2010
Received in revised form 30 August 2010
Accepted 3 September 2010
Available online 21 September 2010

Keywords:
Particle size distribution
Superficially porous particle

ABSTRACT

The separation efficiency and kinetics of several commercial HPLC particle types (both fully porous and superficially porous) have been investigated using a pharmaceutical weakly basic N-containing compound as a test molecule. A strong trend between the particle size distribution (PSD) of the particles and the typically employed "goodness of packing"-parameters was observed. The relative standard deviation of the PSD of the tested particles ranged between 0.05 and 0.2, and in this range, a near linear relationship between the A-term constant, the h_{min}-value and the minimal separation impedance was found. The experimental findings hence confirm the recent observations regarding the relationship between the narrow PSD of the recently commercialized porous-shell particles and their superior efficiency and kinetic performance. The outcome also suggests that the performance of the current generation of fully porous particle columns could be significantly improved if the PSD of these particles could be reduced.

1. Introduction

It is commonly accepted that the particle size distribution (PSD) of packed columns used in high-performance liquid chromatography (HPLC) has a large influence on their chromatographic performance [1–4]. Although intuitively it seems preferable to use particles with a narrow size distribution and commercial literature also often presents narrow particle size distributions as "desirable" [2], little scientific literature is available to support this statement.

Early studies have demonstrated that the width of the particle size distribution does not influence the efficiency and permeability of a support as long as it is not wider than 40% around the mean [1]. Dewaele and Verzele studied the effect of an increasing particle size distribution by mixing two batches of different particle sizes together in different ratios [2]. They found that a large PSD had no influence on column efficiency if the eluting speed was kept around the optimum velocity, while at higher flow rates a small negative effect was observed. Because the A-term contribution was not affected by a greater particle size distribution, the authors concluded that improvements in chromatographic results should not be expected from smaller particle size distributions. Similar observations were made by Endele et al. [3], who obtained values for the A-term contribution of porous silica particles (5–35 μm) that were independent of the PSD width (σ = 0.1–0.25) of the packings.

However, these authors interpreted their plate height data by reducing them with an equivalent sphere diameter, based on the experimentally measured column permeability and the assumption that the flow resistance factor is equal for particles from the same origin as well as their mixtures.

It must be remarked that there is no theoretical foundation for the employed equivalent sphere diameter approach (which is based on the questionable assumption that the flow resistance is independent of the PSD). Given that it can be assumed that a mixture of particles with a widely differing diameter will give rise to a packing structure wherein the small particles settle in the through-pores formed around the largest particles, hence more or less blocking these larger through-pores, it can be inferred that this packing will have a different "shape" or flow resistance than that of a pure particle batch. Therefore, the conclusions of the Dewaele and Verzele-paper might be biased.

Since these early studies, a lot has moreover changed in the landscape of particle manufacturing. Much effort has been dedicated to improve column packing strategies, resulting in more reproducible and overall better performing columns. With the advent of the sub-2 μm particles, which have proven to be more difficult to produce homogeneously [5], the importance of a narrow PSD has become a timely topic again.

To re-evaluate the results from Dewaele and Verzele [2], a similar study was repeated by mixing two batches of 1.7 and

* Corresponding author. Tel.: +32 2 629 33 30; fax: +32 2 629 32 48.
E-mail address: dcaboote@vub.ac.be (D. Cabooter).

0021-9673/$ – see front matter © 2010 Elsevier B.V. All rights reserved.
doi:10.1016/j.chroma.2010.09.008

Table 1
Chromatographic conditions and experimental data relevant to the evaluated columns.

Column	Mobile phase (acetate buffer/ACN)	Mobile phase viscosity (mPa s)[a]	Diffusion coefficient ($\times 10^{-10}$ m^2/s)	Retention factor (k_{G1})	Permeability ($\times 10^{-14}$ m^2)[b]
XBridge	37/63	0.52	5.8	4.6	1.73
Hypersil Gold	41/59	0.54	5.3	4.7	1.82
Gemini NX	34/66	0.50	5.8	4.4	1.98
ACE3	35/65	0.50	5.7	4.7	1.48
Kinetex	38/62	0.52	5.5	4.7	1.18
Halo	36/64	0.51	5.7	4.4	1.02
Poroshell	36/64	0.51	5.7	4.7	0.99

[a] Values calculated from [16].
[b] Values calculated from experimental data at maximum operated pressure and 40 °C.

2.2 μm material in different ratios and subsequently evaluating the chromatographic performance of the columns packed with these particle mixtures [6]. These chromatographic results were subsequently compared with the PSDs obtained by Coulter counting measurements. Because no clear relation was obtained between the observed chromatographic performance and the width of the PSD of the different columns, it was concluded that there was no direct relation between the span of the PSD and the packing quality. The only significant effect that could be observed was related to the number of fines in the particle mixtures. When this number was high, the kinetic performance of the columns was worse and vice versa. This could be explained by the fact that these fines are able to position themselves between the larger particles, in this way increasing the flow resistance of the packing material.

The width of the PSDs obtained for these columns, however, was in the rather narrow range of $\sigma = 0.19–0.26$. This limited range might have made it difficult to see a clear relationship between PSD and minimum reduced plate height.

More recent studies, focused on particles with a different design such as the superficially porous particles, have suggested that particles displaying a very narrow PSD can lead to unprecedented low minimal plate heights [7,8]. It is however unclear whether this finding can be purely related, because there are also other factors that might influence the packing quality. Superficially porous particles for example have a higher density and some of them are rougher than fully porous particles [7,9]. This might also have had an influence on the achieved packing quality, apart from the PSD. Computer simulations [10] have also suggested that narrower particle size distributions result in more homogeneous packed beds of higher efficiency.

In the present study, we compared several commercially available supports (both fully porous and porous-shell materials) from different manufacturers on the basis of some of the commonly used "packing quality" measures such as the value of the minimal plate height and the value of the A-term constant. The width of the PSDs of these columns covers a larger range ($\sigma = 0.06–0.21$) than the study described above [6]. Although the relation between these measures and the true "packing quality" (whatever that may be) is by no means exact or theoretically sound, we report the value of these commonly used packing quality measures here because these are the parameters that are most often considered by the daily practitioners in the field. To make really conclusive statements about the packing quality, an in situ geometrical analysis of how the particles are packed in the column would be needed.

2. Experimental

2.1. Chemicals and columns

Uracil (≥99%), acetonitrile (gradient grade), ethanol (analytical grade) and acetic acid (glacial, 99.8%) were purchased from Sigma–Aldrich (Steinheim, Germany). Ammonium acetate (ACS, reagent) was purchased from Merck (Darmstadt, Germany). Deionized water (≤0.055 μS) was produced by MilliQ equipment (Millipore, Molsheim, France). The pharmaceutical compound was kindly provided by GlaxoSmithKline (Verona, Italy). The compound that will be referred to as G1 in the remainder of the text is an N,N-derivatised piperidine, containing a pyridine moiety. Its main physicochemical characteristics are: molecular weight 669 Da, pK_a 2.0 and 5.0 (measured from solubility data in saturated conditions and fitted by Kaleida Graph software), LogD 5.7 (measured as Log of the distribution coefficient between aqueous phase buffered at pH 7.4 and n-octanol).

The following columns were evaluated: an XBridge C18 column (150 mm × 4.6 mm, 3.5 μm) from Waters (Milford, MA, USA), a Gemini NX C18 column (150 mm × 4.6 mm, 3.0 μm) and a Kinetex Fused Core C18 column (100 mm × 4.6 mm, 2.6 μm) from Phenomenex (Torrance, CA, USA), a Hypersil Gold C18 column (150 mm × 4.6 mm, 3.0 μm) from ThermoFisher Scientific (Cheshire, UK), an ACE3 C18 column (150 mm × 4.6 mm, 3.0 μm) from Advanced Chromatography Technology (Aberdeen, UK), a HALO Fused Core C18 column (100 mm × 4.6 mm, 2.7 μm) from Advanced Materials Technologies (Wilmington, DE, USA) and a Poroshell 120 column (100 mm × 4.6 mm) from Agilent (Agilent Technologies, Little River, DE, USA).

2.2. Apparatus and methodology

All experiments were conducted in the isocratic mode. The mobile phase was 10 mM ammonium acetate buffer adjusted to pH 4.5 with aqueous ammonia. The ratio of aqueous buffer and organic modifier was adapted to provide about the same retention factor for the test molecule ($k' \cong 4.7$) on the different columns. Table 1 shows the mobile phase composition and its viscosity, together with the obtained retention factor and diffusion coefficient for G1 on every column. The diffusion coefficient was calculated using the Wilke-Chang equation for the specific mobile phase composition used for every column [11].

The molecule was neutral in all the mobile phases used, despite the fact that the pH of the aqueous buffer (pH = 4.5) before mixing with the organic modifier (acetonitrile) was lower than the molecule's pK_a-value ($pK_a = 5.0$). This is due to the change of the degree of ionization of the molecule in the hydro-organic environment, with respect to its ionization in pure water, upon the addition of ~60% of acetonitrile [12,13]. The neutral state of the molecule in the various mobile phases was also confirmed by both UV spectra in aqueous-organic mixtures and by the trend of the retention time recorded at different buffer pH (data gathered from GlaxoSmithKline, not shown here). Column loading of the test compound was 2.0 μg for all the columns. In the above described elution conditions, absent or negligible ionic interactions between the weakly basic molecule and the stationary phase are expected [14,15]. This is further confirmed by peak tailing values that were recorded for each single experiment and that never exceeded the 0.90–1.10 interval for all the columns.

Van Deemter curves were constructed for every column at a temperature of 40 °C. Every van Deemter curve was measured in triplicate by increasing the flow rate from 0.3 mL/min until the maximum pressure of the system was reached and then repeating the same process two more times. This approach allows checking for column damage that might result from use at the highest flow and pressure. The viscosities of the used mobile phases were calculated according to Li and Carr [16]. The permeability of the columns was determined using Darcy's law, by measuring the pressure drop over the column at the highest linear velocity and is also shown in Table 1 [17]. Peak variances were calculated using the peak width at half height.

The experiments were performed on an Agilent 1100 HPLC system (Agilent Technologies, Waldbronn, Germany) equipped with a variable wavelength UV detector (14.0 μL flow cell, 10 mm path length), a thermostatted column compartment and a quaternary pump. All connection tubing (diameter 120 μm) was kept as short as possible to reduce extra-column band broadening. The total volume of the systems was determined to be 37 μL. The system was operated with Empower software. The maximum pressure on this system is 400 bar.

Samples consisting of 500 μg/mL uracil and 400 μg/mL G1 were dissolved in 50/50 (v%/v%) water/acetonitrile. The injected sample mixture volume was 2 μL. Absorbance values were measured at 260 nm with a sample rate of 40 Hz (response time: 0.1 s). This was the maximum sample rate available on the instrument.

All reported plate height and column permeability data were obtained after correction for the system band broadening (σ^2_{sys}), t_0-time (t_{sys}) and pressure drop (ΔP_{sys}), measured using G1 as probe molecule and by removing the column from the system and replacing it with a zero-dead volume connection piece, under the same experimental conditions as for the plate height measurements [18,19]:

$$N_{col} = \frac{(t_{R,total} - t_{R,sys})^2}{\sigma^2_{total} - \sigma^2_{sys}} \quad (1)$$

$$H_{col} = \frac{L}{N_{col}} \quad (2)$$

$$K_{v0} = \frac{u_0 \eta L}{\Delta P_{total} - \Delta P_{sys}} \quad (3)$$

Under the current experimental conditions ($k' \approx 5$) and using the columns in a 4.6 mm i.d. format, the losses in efficiency, caused by the system contribution never exceeded more than 5%. These findings are in excellent agreement with [19].

The experimental van Deemter data were fitted in MatLab (The MathWorks Inc., Natick, MA, USA). The same software was used to assess the confidence intervals (95%) of the fitted parameters and the overall quality of the fitting.

2.3. Particle analysis

To determine the true particle size of the studied columns, the columns were opened after the separation experiments and the particles were removed by gently flushing the columns with ethanol. The particles were subsequently dried by evaporating the ethanol at room temperature in the fume hood and prepared for SEM (scanning electron microscopy) measurements. The SEM pictures were recorded with a Quanta FEG 200 instrument equipped with a Field Emission Gun source. The microscope was operated at 20 kV with a magnification of 3500× and a backscattered electrons detector (BSED) to obtain enhanced contrast conditions. The particles were conductive enough to omit the use of a conductive coating layer and they were analyzed onto a self adhesive carbon sample holder. At least 4 pictures of each sample were taken and 800 particle diameters were measured for every column by re-processing the images with the CLEMEX PS[3] image analysis software in order to determine the true particle size.

Table 2
Particle diameters specified by the manufacturer, number-averaged ($d_{p,\#}$) and Sauter-mean ($d_{p,SA}$) particle sizes and standard deviation of the particle size distribution of the different supports, obtained from SEM images.

Column	Manufacturer's d_p (μm)	$d_{p,\#}$ (μm)	Stdev PSD (σ)	$d_{p,SA}$ (μm)
XBridge	3.5	3.9	0.21	4.2
Hypersil Gold	3.0	4.0	0.16	4.3
Gemini NX	3.0	3.4	0.19	3.6
ACE 3	3.0	3.5	0.13	3.6
Kinetex	2.6	2.7	0.06	2.7
Halo	2.7	2.8	0.10	2.8
Poroshell	2.7	2.7	0.07	2.7

3. Results and discussion

3.1. Particle analysis

The performance of four traditional fully porous particle supports with particle sizes ranging between 3.0 and 3.5 μm (ACE3, Gemini NX, Hypersil Gold and XBridge) and three superficially porous columns with particle sizes of 2.6–2.7 μm (Kinetex, HALO and Poroshell 120), all with a C_{18} stationary phase, was evaluated at pH = 4.5 using G1 as test compound. For this purpose, plate heights were measured at flow rates ranging between 0.3 mL/min and the maximum flow rate that could be obtained at 400 bar on each column. In order to assess the performance of the columns in an independent way, an accurate knowledge of the average particle diameter of every support was necessary. Therefore, SEM pictures were taken from loose packing material of every column and these pictures were subsequently processed with image analysis software. Fig. 1 shows SEM pictures for particles of every support type.

Among the fully porous particles (Fig. 1a–d), the greatest homogeneity is observed for ACE3, whereas the XBridge (Fig. 1a) and certainly also the Gemini NX (Fig. 1d) batches include some particles with a size that is noticeably larger than the average particle size.

Comparing the fully porous particles with the superficially porous particles (Fig. 1e–g) the latter are clearly smaller than the former and also display a greater homogeneity. Little difference in size and homogeneity is moreover observed among the superficially porous particles.

From the SEM pictures, the number-average particle diameters were determined to be 2.7 μm for Kinetex and Poroshell, 2.8 μm for Halo, 3.9 μm for the XBridge support, 4.0 μm for Hypersil Gold, 3.4 μm for Gemini NX and 3.5 μm for ACE3. These values are shown in Table 2. For the fully porous particles, the values obtained are clearly larger than the values specified by the manufacturers. This might be related to the fact that different techniques (e.g. Coulter counting, which is known to underestimate the size of fully porous particles [20]) were used to determine the average particle diameter.

The particle size distribution of the different supports was subsequently determined from the same data by expressing the diameter of at least 800 particles per column batch in a frequency distribution diagram. To properly normalize the graph (surface under curves should be unity), the results were plotted as $d_{p,i}/d_{p,average}$ versus $d_{p,average} \times n_i/(n_i \times \Delta d_{p,i})$ [21], with the $\Delta d_{p,i}$ the width of the intervals in the PSD, in this case chosen to be 0.2 μm. The resulting distribution plots are shown in Fig. 2.

From the distribution plots in Fig. 2, it is evident that the superficially porous particles indeed have a much narrower particle size

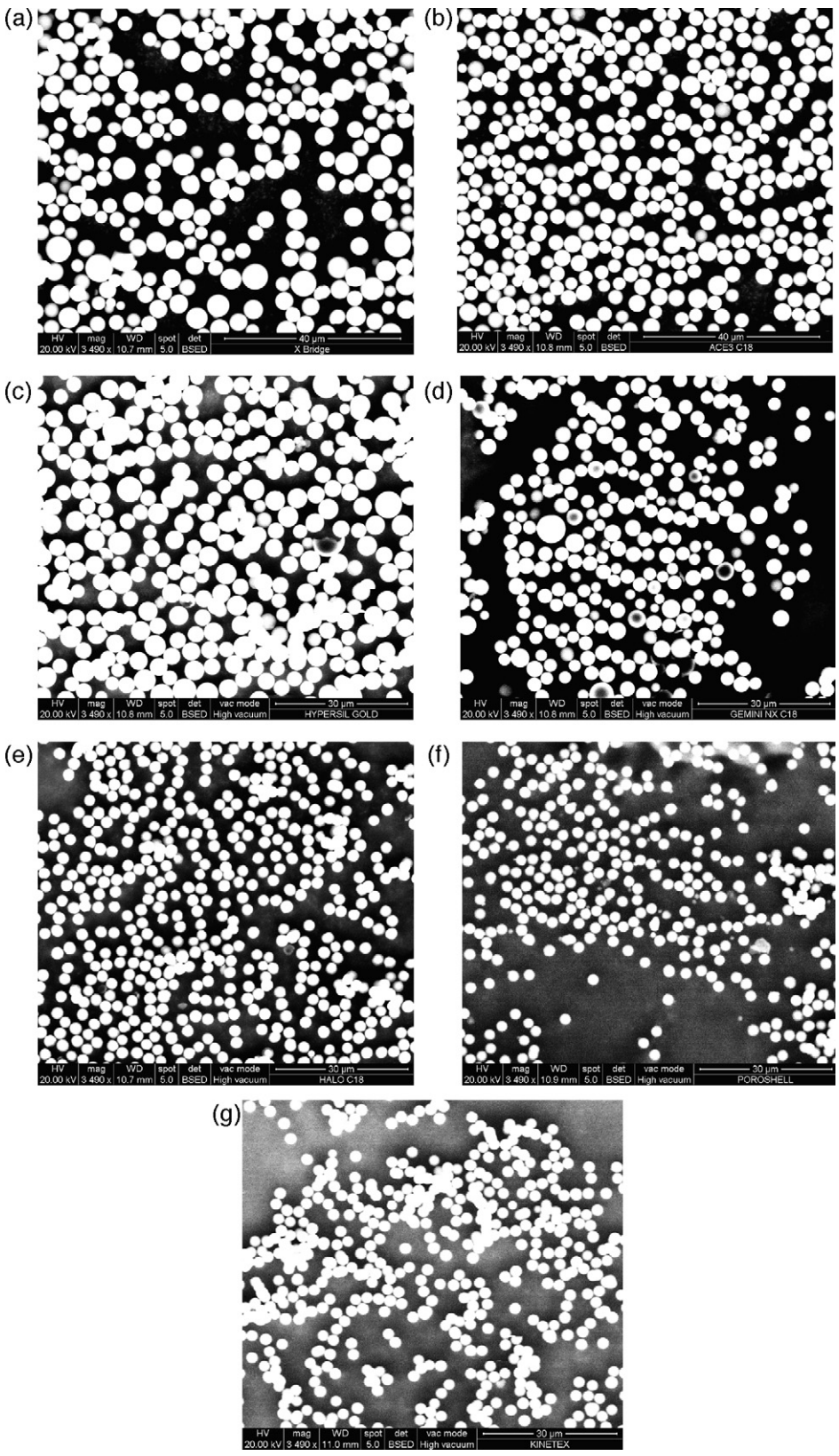

Fig. 1. SEM pictures obtained for the different packings: (a) XBridge, (b) ACE 3, (c) Hypersil Gold, (d) Gemini NX, (e) HALO Fused Core, (f) Poroshell and (g) Kinetex Fused Core. The microscope was operated at 20 kV with a magnification of 3500× and a backscattered electrons detector (BSED) to obtain enhanced contrast conditions.

distribution than the fully porous supports, as was already obvious from the SEM pictures. Highly controlled processes for the generation of the particles are probably responsible for the very narrow particle size distributions of these particles [22,23]. Among the fully porous supports, the ACE3 column has the narrowest PSD, while the XBridge column has the broadest PSD. The Gemini NX and Hypersil Gold columns have a similar PSD, displaying a width somewhere between that of the ACE3 and XBridge PSD curves.

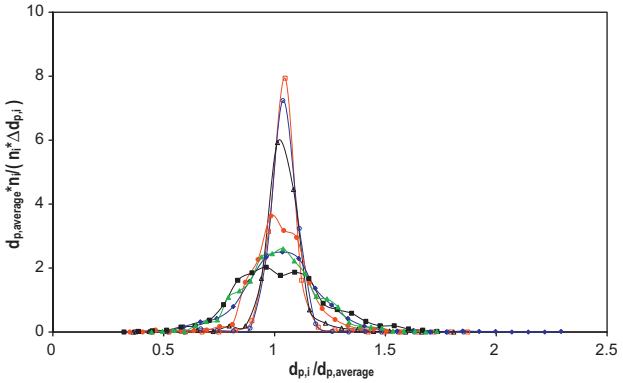

Fig. 2. Normalized particle size distributions of the different evaluated support types, determined from SEM pictures. XBridge C_{18} (d_p = 3.5 μm) (■), ACE3 C_{18} (d_p = 3.0 μm) (●), Gemini NX C_{18} (d_p = 3.0 μm) (◆), Hypersil Gold C_{18} (d_p = 3.0 μm) (▲), Kinetex Fused Core C_{18} (d_p = 2.6 μm) (□), HALO Fused Core C_{18} (d_p = 2.7 μm) (△) and Poroshell C_{18} (d_p = 2.7 μm) (○).

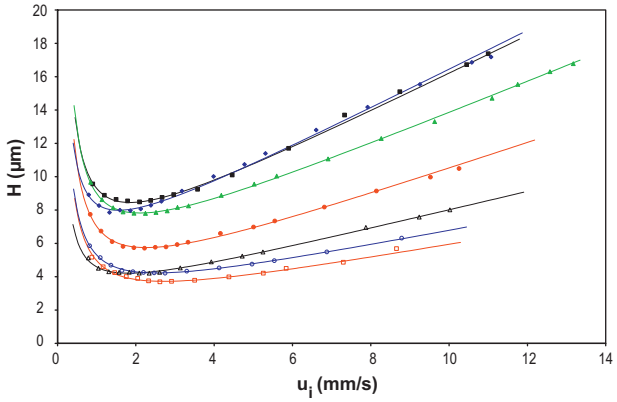

Fig. 3. Plate height curves of interstitial velocity (u_i) versus plate height (H) obtained for the pharmaceutical test compound on the different evaluated support types. The mobile phase consisted of water (10 mM ammonium acetate, pH = 4.5) and acetonitrile in a ratio that lead to the same retention factor for the test compound on all investigated supports (k' = 4.6 ± 0.2). Symbols are the same as in Fig. 2.

To represent the width of the PSD in a more quantitative way, the standard deviations of the distribution plots in Fig. 2 were calculated from their 0th (MOM_0), 1st (MOM_1) and 2nd (MOM_2) order moment as follows:

$$\sigma = \sqrt{\frac{MOM_2}{MOM_0} - \left(\frac{MOM_1}{MOM_0}\right)^2} \quad (4)$$

The obtained standard deviations are shown in Table 2 and are very similar to the standard deviations that are cited in literature for both superficially porous ($\sigma \cong 0.05$) and fully porous particles ($\sigma < 0.25$) [4,7,24,25]. The values are in perfect agreement with the order of the curves in Fig. 2, with the broadest curves producing the largest standard deviation. One might suspect an artifact in the moment calculation for the Gemini NX and the Hypersil Gold particles, who both display a similar width in Fig. 2, while yet the former leads to a slightly larger σ. The observed difference in σ can however readily be explained by the presence of relatively large particles ($d_p = 1.8 \times d_{p,average}$) in the tail of the PSD curve for the Gemini NX particles (blue curve), whereas this does not occur for the Hypersil Gold particles (for interpretation of the references to color in this sentence, the reader is referred to the web version of the article).

3.2. Performance evaluation and packing quality of the tested supports

Fig. 3 shows experimentally obtained plate height curves for the test molecule on the different evaluated support types. Because both fully porous and superficially porous columns – with different porosities – are being compared, the plate height curves have been constructed using the interstitial velocity instead of the linear velocity. The plate height curves clearly show the expected behaviour in efficiency as a function of particle size, independent of the support type. The 2.6–2.7 μm columns display lower plate height values than the 3.0–3.5 μm supports.

Focusing on the traditional fully porous 3.0–3.5 μm support types (full lines and symbols), Fig. 3 shows that a clear distinction in performance can be made between the Gemini, Hypersil and XBridge columns on one hand, and the ACE3 column on the other hand. Whereas Gemini (d_p = 3.0 μm) and Hypersil (d_p = 3.0 μm) have a minimum plate height of 7.7 μm and XBridge (d_p = 3.5 μm) has a minimum plate height of 8.5 μm, the ACE3 column (d_p = 3.0 μm) clearly performs better with a minimum plate height of 5.8 μm.

Considering subsequently the superficially porous particles, the Kinetex column (d_p = 2.6 μm) has a slightly lower minimum plate height than the Poroshell and Halo columns (both d_p = 2.7 μm), again in agreement with the slightly smaller particle size of the Kinetex particles.

With an accurate knowledge of the particle sizes of the different supports, the obtained plate height measurements can be properly reduced and used to evaluate the performance of the columns both in terms of efficiency and, as generally accepted, packing quality. Using the number-averaged particle diameters obtained from the analysis of the SEM pictures of each packing type, the reduced plate height plots in Fig. 4 were constructed. The experimental data were fitted using the van Deemter equation [26]:

$$h = A + \frac{B}{v} + Cv \quad (5)$$

where h is the reduced plate height, v is the reduced interstitial velocity and A, B and C are the van Deemter parameters. The obtained van Deemter parameters are shown in Table 3, together with their confidence intervals and the quality of the fit. The minimum reduced plate heights determined from the reduced plate height plots are also shown in Table 3.

From the reduced plate height curves shown in Fig. 4, it is clear that the Kinetex column provides the lowest reduced plate heights (thus suggesting the best packing quality), followed closely by the HALO and Poroshell supports. Interestingly, the ACE3 has a reduced plate height curve that is nearly as good as that of the superfi-

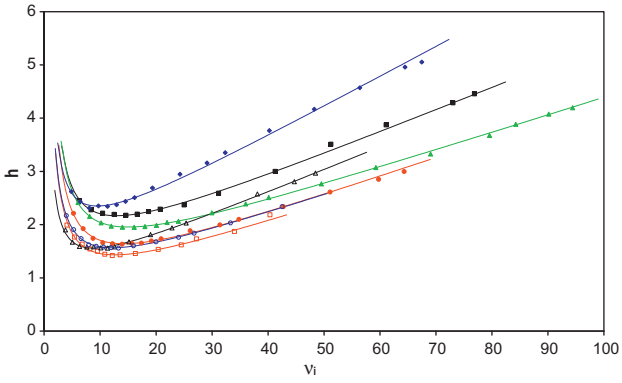

Fig. 4. Reduced plate height plots obtained for the pharmaceutical test compound on the supports evaluated in Fig. 3. The mobile phase consisted of water (10 mM ammonium acetate, pH = 4.5) and acetonitrile in a ratio that lead to the same retention factor for the test compound on all investigated supports (k' = 4.6 ± 0.2). Symbols are the same as in Fig. 2.

Table 3
Van Deemter parameters obtained by fitting the experimental plate height data with Eq. (5) and minimum reduced plate heights of the evaluated columns. The confidence intervals and quality of the fit (R^2) are also given.

Column	A	B	C	R^2	h_{min}
XBridge	1.04 (±0.10)	7.26 (±0.90)	0.04 (±0.00)	0.9979	2.18
Hypersil Gold	0.94 (±0.04)	7.96 (±0.35)	0.03 (±0.00)	0.9995	1.95
Gemini NX	1.17 (±0.06)	5.84 (±0.46)	0.06 (±0.00)	0.9948	2.31
ACE 3	0.75 (±0.08)	6.55 (±0.61)	0.03 (±0.00)	0.9948	1.63
Kinetex	0.54 (±0.10)	5.41 (±0.58)	0.03 (±0.00)	0.9807	1.37
HALO	0.74 (±0.05)	3.61 (±0.28)	0.04 (±0.00)	0.9983	1.52
Poroshell	0.69 (±0.04)	5.35 (±0.19)	0.04 (±0.00)	0.9979	1.56

cially porous supports. The other fully porous supports follow the same ranking as in Fig. 3, except for the Gemini NX and XBridge columns, that have switched places due to the small particle size of the Gemini packing.

From Table 3, it can also be observed that the superficially porous particles have a B-term contribution that is slightly lower than that of the fully porous particles. This is because diffusion is more hindered by the presence of the solid core inside the superficially porous particles compared to the fully porous particles [24].

Another way to assess the packing quality of a support is by using a so-called reduced kinetic plot, plotting the separation impedance (E) versus N/N_{opt} [6,27]. Both measures can be calculated without having to define a characteristic length or diameter, as can be seen in the following equations:

$$E = \frac{H^2}{K_V} = \frac{h^2}{\phi} \tag{6}$$

$$\frac{N}{N_{opt}} = \frac{u_{opt}H_{min}}{uH} = \frac{v_{opt}h_{min}}{vh} \tag{7}$$

with ϕ the flow resistance ($\phi = d_p^2/K_v$)

A reduced kinetic plot can be analyzed in the same way as a reduced plate height curve: the lower the curve the better the intrinsic quality of the particles and the packing. However, whereas the reduced plate height curve only represents the efficiency, the reduced kinetic plot also incorporates information on the flow resistance of the support, as can be seen from Eqs. (6) and (7), and hence is a direct measure for the overall kinetic performance of a given support type.

When using a reduced kinetic plot curve to assess the "goodness" of the packing, it should be realized that the permeability constant K_{v0} used in Eq. (6) also partly depends on the intra-particle porosity. To filter out the effect of any differences in intra-particle porosity that exist between the different supports under evaluation, the separation impedance (E_i) should be based on the permeability that is based on the interstitial velocity rather than on the linear velocity [4]. In the present study, E_i was calculated starting from the experimentally obtained values of the permeability based on the linear velocity (K_{v0}, determined with Eq. (3), see Table 1) as follows:

$$E_i = \frac{H^2}{K_{Vi}} = \frac{H^2}{K_{v0}}\frac{\varepsilon_e}{\varepsilon_T} \tag{8}$$

where ε_T is the total porosity of the support and ε_e is the external or interstitial porosity.

The total porosity of the columns was determined from the elution time of uracil [28], injected together with G1 under the same mobile phase conditions, after correction for the extra-column contribution, and is shown in Table 4. The values of the external porosity (ε_e) were derived from the experimentally obtained permeability (K_{v0}) and ε_T values using Kozeny-Carman's law:

$$K_{v0} = \frac{d_{p,SA}^2}{f_{KC}}\frac{1}{\varepsilon_T}\frac{\varepsilon_e^3}{(1-\varepsilon_e)^2} \tag{9}$$

Where the Kozeny constant (f_{KC}) was assumed to be 180 [21] and $d_{p,SA}$ is the Sauter-mean diameter, defined as:

$$d_{p,SA} = \frac{\sum d_{p,i}^3}{\sum d_{p,i}^2} \tag{10}$$

For the determination of the Sauter-mean diameter, the nominal particle sizes ($d_{p,i}$) of the packing materials obtained from the SEM pictures elaborated by the image analysis software, were used. Table 2 lists the Sauter-mean diameters of the different packing materials.

It must be remarked here that even though it is suggested in some studies that the number-averaged particle size should be used for the characterization of the mean particle size of a particle batch [4], the original derivation of the Kozeny-Carman law [29] clearly implies that the mean particle diameter should be based on the specific contact surface between the particles and the liquid, i.e., on the Sauter-mean diameter as defined in Eq. (10). This is a direct consequence of the physics of the problem, which is that of a driving force for a volumetric fluid flow countered by the flow arresting force originating from the stationary particle surfaces.

Table 4 shows the obtained values for the external porosities of the columns. ACE3 and Hypersil have a similar ε_e of 0.360 and 0.363, respectively. The XBridge column has a much lower ε_e-value of 0.341 indicating that this column is very densely packed. Similar small external porosity values have already been observed for other column types from the same manufacturer [21]. The Gemini NX column is clearly less densely packed than the other fully porous columns, having an external porosity value of 0.383. The superficially porous particles have slightly higher external porosities than the fully porous particles, an observation that was also made in [9,30] and was explained by the larger rugosity of the superficially porous particles, causing friction between the particles that prevents a dense packing.

From the obtained values for ε_T and ε_e the internal porosity of the packings can be calculated as:

$$\varepsilon_i = \frac{\varepsilon_T - \varepsilon_e}{1-\varepsilon_e} \tag{11}$$

The obtained values of ε_i are shown in Table 4 and show that the superficially porous particles have a significantly lower internal porosity than the fully porous particles, a difference that can in part

Table 4
Experimentally determined permeability (K_{v0}), porosity (ε) and minimum separation impedance values of the evaluated columns.

Column	ε_T	ε_e	ε_i	$E_{i,min}$
XBridge	0.54	0.34	0.30	0.30
Hypersil Gold	0.66	0.36	0.47	0.47
Gemini NX	0.52	0.38	0.22	0.22
ACE 3	0.55	0.36	0.30	0.30
Kinetex	0.51	0.39	0.21	0.21
Halo	0.45	0.38	0.12	0.12
Poroshell	0.52	0.37	0.23	0.23

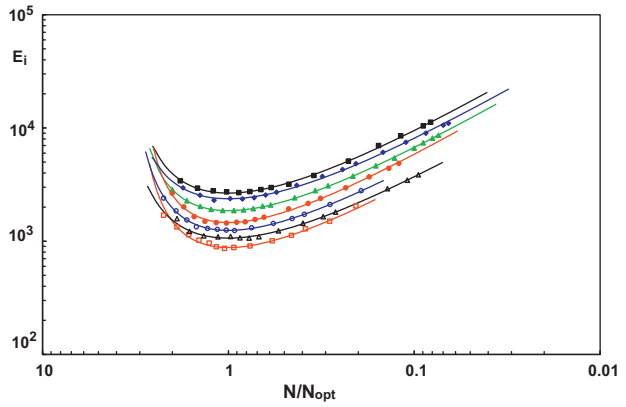

Fig. 5. Reduced kinetic plots of E_i versus N/N_{opt} obtained for G1 on the supports evaluated in Fig. 3. Same symbols are used as in Fig. 2.

be explained by the presence of the solid core in the superficially porous particles [9].

With the obtained values of ε_T and ε_e the impedance plots based on the interstitial velocities shown in Fig. 5 were constructed. The order of the curves in Fig. 5 remains largely the same as in the reduced plate height plots shown in Fig. 4. Only the order of the XBridge and Gemini NX has shifted again. The most important difference between the plots shown in Figs. 4 and 5 is that the latter also incorporates information on the permeability of the support. From Table 1, it is evident that the Gemini NX column has a much larger permeability than the XBridge column, despite the fact that the latter has a larger average particle diameter. This has certainly to do with the larger external porosity value of the Gemini NX column, resulting in a less dense and hence more permeable packing.

3.3. *Relation between particle size distribution and quality packing parameters*

To investigate the relationship between the width of the particle size distribution on the one hand and the quality of the packing and efficiency of the thus obtained support on the other hand, the standard deviations obtained for the different supports were compared with several dimensionless parameters that generally can be considered as a measure for the quality of a packing.

A first parameter that can be used to assess the packing quality of a support, independent of the size of the particles, is the minimum plate height (h_{min}). To relate the particle size distribution of the supports to their packing quality, plots of h_{min} versus the standard deviation of the PSD (σ) are shown in Fig. 6a. From these plots, a clear linear relationship between h_{min} and the width of the PSD is evident. For the sake of interest, the data obtained in [6] have also been added to this figure (open, red symbols) (for interpretation of the references to color in this sentence, the reader is referred to the web version of the article). As can be seen from Fig. 6a, the particles from [6] follow the same linear relationship between h_{min} and σ, a trend that was obviously not so clearly visible when a smaller range of PSD widths was investigated.

A second traditionally employed measure for packing quality is the A-constant of the reduced van Deemter curve. The band broadening that emerges from the tortuosity of the flow paths, caused by inhomogeneities in the packing, will mostly be reflected in this term. Therefore, it was also considered useful to relate the standard deviation of the PSD of the different packings to the value of the A-term constant (Fig. 6b). Again, a significant linear trend between the A-term constant and σ can be seen. The A-term values obtained for the particles studied in [6] have again been added to this figure and can be seen to follow the same trend as well.

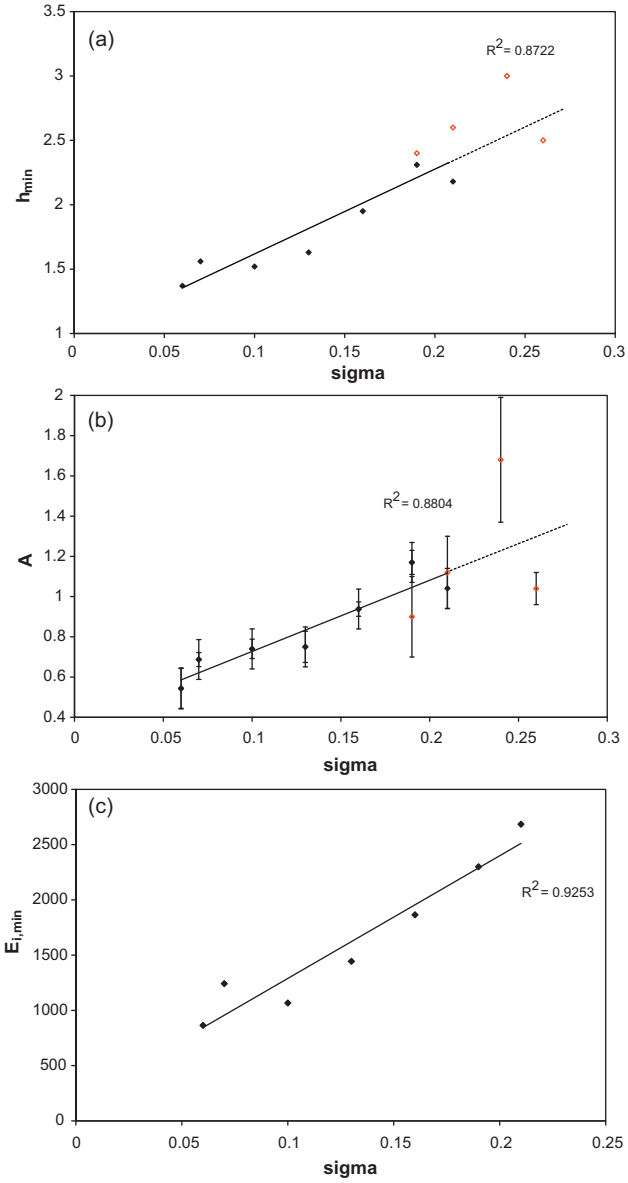

Fig. 6. (a) Plot of h_{min} versus sigma (width of the PSD) and (b) A versus sigma for the particles studied in the present manuscript (full symbols) and for the particles studied in [6] (open symbols) and (c) plot of $E_{i,min}$ versus sigma for the supports evaluated in Figs. 3–5. The full line represents the trend line that was obtained for the full symbols, while the dashed line is the same, extrapolated trend line. The confidence intervals obtained for the A-values are also shown in b.

At third parameter that can be used to assess the quality of a packing, is the minimum separation impedance ($E_{i,min}$) as determined from the curves in Fig. 5 (see Table 4): the lower the minimum separation impedance of a support, the better the intrinsic quality of the particles and the packing. Plots of $E_{i,min}$ versus sigma are shown in Fig. 6c where again a clear linear relationship with σ can be observed for all columns. Compared to the other two packing quality measures (cf. Figs. 6a and b), the minimum separation impedance leads to the clearest linear relationship (highest R^2-value) with the width of the particle size distribution.

4. Conclusions

A strong (nearly linear) correlation has been observed between the width of the particle size distribution of several commercially

available HPLC particle types (both fully porous and superficially porous) and some commonly used parameters that reflect the quality of a packing, namely the minimum reduced plate height, the A-term and the minimum reduced separation impedance. These observations have been made despite the fact that the studied particles have a number of other differences besides PSD, such as particle porosity, pore size, pore structure and bonding conditions.

Covering a wide group of fully porous as well as porous-shell particles, these observations confirm the most recent views in the field, stating that there is a strong relation between the particle size distribution of the packings and the quality of the packing. The observed nearly linear relationship also suggests that the performance of the current generation of fully porous particle columns could be significantly improved if the PSD of these particles could be reduced.

The current data are compared on the basis of common column lengths and column internal diameters. No considerations can be indirectly drawn for different packing formats, because additional and different variables affecting packing quality should be evaluated experimentally and analyzed. This is enforced by the evidence that certainly not only the PSD plays a role in the final packing quality, but also the procedure used for the packing of the columns. To make really conclusive statements about the packing quality, an in situ geometrical analysis of how the particles are packed in the column would be needed.

Acknowledgements

Dionigio Franchi, Director of Pharmaceutical Development, GSK Verona R&D (Italy), is sincerely acknowledged for effectively and enthusiastically supporting the present work. Deirdre Cabooter is a Postdoctoral Fellow of the Research Foundation Flanders (FWO Vlaanderen).

References

[1] I. Halasz, M. Naefe, Anal. Chem. 44 (1972) 76.
[2] C. Dewaele, M. Verzele, J. Chromatogr. 260 (1983) 13.
[3] R. Endele, I. Halasz, K. Unger, J. Chromatogr. 99 (1974) 377.
[4] U.D. Neue, HPLC Columns: Theory, Technology and Practice, Wiley-VCH, New York, 1997.
[5] F. Gritti, G. Guiochon, J. Chromatogr. A 1217 (2010) 1485.
[6] J. Billen, D. Guillarme, S. Rudaz, J.-L. Veuthey, H. Ritchie, B. Grady, G. Desmet, J. Chromatogr. A 1161 (2007) 224.
[7] J.J. DeStefano, T.J. Langlois, J.J. Kirkland, J. Chromatogr. Sci. 46 (2008) 254.
[8] F. Gritti, I. Leonardis, J. Abia, G. Guiochon, J. Chromatogr. A 1217 (2010) 3819.
[9] F. Gritti, A. Cavazzini, N. Marchetti, G. Guiochon, J. Chromatogr. A 1157 (2007) 289.
[10] J. Billen, P. Gzil, F. Lynen, P. Sandra, P. van der Meeren, G. Desmet, Poster presentation, HPLC 2006, San Francisco, CA, June 2006.
[11] A. Fanigliulo, D. Cabooter, G. Bellazzi, B. Allieri, A. Rottigni, G. Desmet, J. Chromatogr. A, (2010), doi:10.1016/j.chroma.2010.08.071.
[12] S. Pous-Torres, J.R. Torres-Lapasio, J.J. Baeza-Baeza, M.C. Garcıa-Alvarez-Coque, J. Chromatogr. A 1163 (2007) 49.
[13] X. Subirats, E. Bosch, M. Rosès, J. Chromatogr. A 1059 (2004) 33.
[14] S.M.C. Buckenmaier, D.V. McCalley, Anal. Chem. 74 (2002) 4672.
[15] N.H. Davies, M.R. Euerby, D.V. McCalley, J. Chromatogr. A 1178 (2008) 71.
[16] J. Li, P.W. Carr, Anal. Chem. 69 (1997) 2530.
[17] D. Cabooter, F. Lestremau, A. de Villiers, K. Broeckhoven, F. Lynen, P. Sandra, G. Desmet, J. Chromatogr. A 1216 (2009) 3895.
[18] D. Guillarme, S. Heinisch, J.L. Rocca, J. Chromatogr. A 1052 (2004) 39.
[19] D.V. McCalley, J. Chromatogr. A 1217 (2010) 4561.
[20] T. Allen, Particle Size Measurement, Chapman and Hall, London, 1968.
[21] D. Cabooter, J. Billen, H. Terryn, F. Lynen, P. Sandra, G. Desmet, J. Chromatogr. A 1178 (2008) 108.
[22] J.J. Kirkland, F.A. Truszkowski, C.H. Dilks, G.S. Engel, J. Chromatogr. A 890 (2000) 3.
[23] E. Abbasi, J. Layne, H. Behr, S. Countryman, Phenomenex Application Note, TN-1069, http://www.phenomenex.com.
[24] F. Gritti, G. Guiochon, J. Chromatogr. A 1166 (2007) 30.
[25] E. Olah, S. Fekete, J. Fekete, K. Ganzler, J. Chromatogr. A 1217 (2010) 3642.
[26] J.J. van Deemter, F.J. Zuiderweg, A. Klinkenberg, Chem. Eng. Sci. 5 (1956) 271.
[27] D. Cabooter, S. Heinisch, J.L. Rocca, D. Clicq, G. Desmet, J. Chromatogr. A 1143 (2007) 121.
[28] F. Gritti, G. Guiochon, J. Chromatogr. A 995 (2003) 37.
[29] J.M. Coulson, J.F. Richardson, Chemical Engineering Volume 2 – Particle Technology and Separation Processes, Pergamon Press, Oxford, UK, 1999.
[30] F. Gritti, G. Guiochon, J. Chromatogr. A 1176 (2007) 107.